

Multirate Adaptive Filter Banks based on Automatic Bands Selection for Epilepsy Detection

Daniel Nieto, Juan D. Martinez-Vargas, Eduardo Giraldo

Abstract—In this paper, a novel methodology that automatically identifies segments of EEG recordings with epileptic activity based on multi-rate adaptive filter banks is presented. As an advantage, the proposed approach accurately tracks parameters variability in the specific frequency band of each filter according to its energy in the spectrogram. To this end, the Shannon energy is used as information criteria for filter variability computed over the time-frequency information of the EEG data. Hence, both time and frequency data variability are considered. The proposed approach is evaluated in a real scenario where the information extracted from the obtained filter bank is used to feed a support vector machine to discriminate between normal and epileptic events. In the obtained results are validated that the proposed adaptive approach outperforms fixed filter bank alternatives.

Index Terms—Epilepsy detection, multi-rate filter banks, adaptive.

I. INTRODUCTION

Detecting epileptiform discharges that appear in EEG (electroencephalography) recordings, is an important component in the diagnosis of epilepsy that provides a valuable understanding of its nature, cause, and location.

Analysis of EEG signals is usually accomplished in temporal or frequency domains. For instance, in [1], [2], authors proposed frequency analysis methods based on power spectra for epileptic seizure detection using multiple signal classification (MUSIC), auto-regressive (AR), and periodogram methods. However, such methods do not consider time information and temporal variability causing a low-accurate detection of epileptiform discharges. As an alternative, several authors have proposed filter-bank based methods that allow analysis in both time and frequency domains [3], [4]. However, in bank analysis, filter bandwidths are fixed, yielding equally weighted frequency bands for further analysis, which is not always true when dealing with epileptic activity over EEG data [5]. As a result, these methods do not take into account the spectral variability in each frequency band. Examples of the above-mentioned methods are wavelets and many other time-frequency representations, which are usually calculated through filter banks [6]. Consequently, such conventional

methods for epilepsy detection do not consider EEG temporal variability [7].

In order to model more adequately the EEG signals behavior, the spatio-temporal dynamics of the brain should be considered [8]. However, in lack of an explicit criterion, temporal analysis is usually performed visually by experts (neurologists) to detect the onset of epileptic seizures. As such analysis may be insufficient and highly depends on the expertise level of the medical team, some studies suggest empirical mode decomposition analysis as a tool to include temporal EEG dynamics into account [9], [10].

However, biological signals have a time-variant structure that demands feature extraction techniques, changing and adapting itself according to the dynamical behavior. In this sense, an important modification of the fixed filters bank analysis consists of modifying filter parameters, particularly its order, that might change according to the dynamical information of the signal. As a result, filter banks with adaptive parameters might track in a more accurate way any change of parameters of a time-varying sequence [11], [12], [13], [14], [15]. Nevertheless, approaches based on filter banks need to tune a set of thresholds for filter order changes. However, the threshold tuning depends on each application. In [14] the thresholds are tuned according to perfect reconstruction criteria, but these methods depend just on the selected filters instead of the analyzed signal. Therefore, it is necessary to develop a dynamic time-varying method to select an automatic threshold that depends on the actual signal [16].

In this work, an adaptive filter bank that varies according to the level energy of the signal is proposed. As an advantage, the method allows a dynamical signal processing structure. In order to get a better description of the time-frequency patterns present in the data in hand, adaptive multi-rate filter banks are proposed for EEG feature extraction [17], using their spectral information. The frequency range of the designed filters change according to the estimated energy level in each sample. To this end, Shannon energy is used as adaptability criteria because: i) it emphasizes the medium-intensity signals and attenuates the effect of low-intensity signals much more than that of high-intensity signals, and ii) the Shannon entropy accentuates the effect of low value noise that makes the envelope too noisy to read. As a result, each frequency band preserves relevant information of the signal. This paper is organized as follows. In section II recalls the theoretical background for multi-rate filter banks and the selection of adaptive multi-rate filters. Finally, in section III are presented the results for epilepsy detection over EEG signals including the tuning of the adaptive multi-rate decomposition and the support vector machines used to solve the classification task.

Manuscript received December 2, 2019; revised October 5, 2020. This work was supported by the Instituto Tecnológico Metropolitano ITM of Medellín-Colombia under Project P20214. Daniel Nieto was founded by DCRI Global office founded by ITM.

Daniel Nieto is a graduated student at the Department of Electrical Engineering, Instituto Tecnológico Metropolitano, Medellín, Colombia, e-mail: danielnieto152326@itm.edu.co

Juan D. Martinez-Vargas is a full professor and researcher at the Department of Electrical Engineering, Instituto Tecnológico Metropolitano, Medellín, Colombia, e-mail: juanmartinez@itm.edu.co

E. Giraldo is a full professor at the Department of Electrical Engineering, Universidad Tecnológica de Pereira, Pereira, Colombia.

Research Group in Automatic Control, e-mail: egiraldos@utp.edu.co.

II. THEORETICAL FRAMEWORK

A. Multi-rate Filter banks

Multi-rate filter banks allows signal decomposition in M frequency bands. Further, each sub-band can be processed to reconstruct solely the events of interest. The process of multi-rate decomposition is as follows: First, data is passed through the analysis bank. Later, the information of interest is extracted in the processing block. Finally, data comprising merely the selected information is reconstructed in the Synthesis bank. The entire process is depicted in Fig. 1.

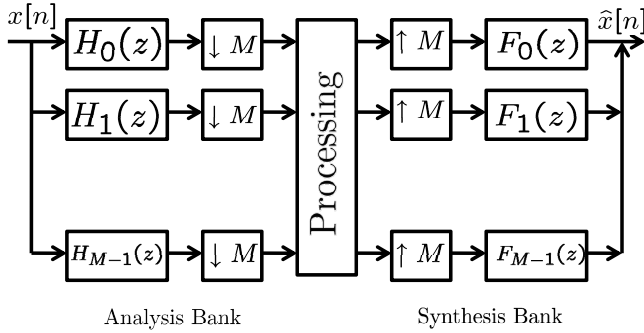


Fig. 1. Multi-rate filter bank

Specifically, the analysis filters $H_k(z)$ split the input signal $x(n)$ into M sub-band signals, which are decimated by a factor M . The synthesis filters $F_k(z)$ interpolate and recombine the M sub-band signals. In Fig. 2 is depicted a multi-rate decomposition for equally distributed filters.

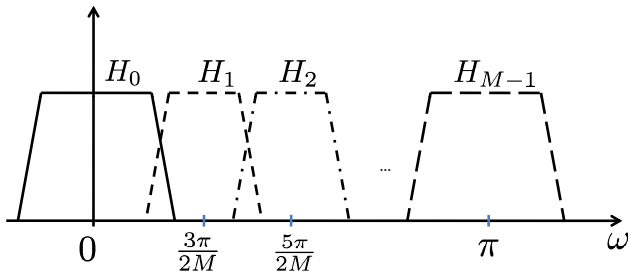


Fig. 2. Ideal frequency for multi-rate filter banks

The decimator and expander that decreases and expand the sampling rate, respectively, are denoted by $(\downarrow M)$ and $(\uparrow M)$. For $M = 2$ orthogonality or biorthogonality conditions are more restrictive than for $M > 2$. This conditions are given in section II-B. The conditions for filter selection can be extended for the case of $M > 2$. However, the number of freedoms grows faster than the number of restrictions. Consequently, the choice of one $M - th$ band filter does not determine the other choices.

B. Mathematical restrictions of filter banks

The conditions for filter selection of a two channel filter bank, in orthogonal and biorthogonal cases, are described as follows. Let $h[n]$ be a FIR filter defined by the sequence $h[n] = \{h[0], h[1], \dots, h[L-1]\}$. For orthogonal filter banks, consider that $h[n]$ is orthogonal to its own translations:

$$\langle h[n-2k], h[n-2l] \rangle = \delta_{kl} \quad (1)$$

where δ_{kl} is the Kronecker delta. Let $H(z)$ be the z -transform of a low-pass filter $h[n]$. Then, a high-pass filter $g[n]$ is defined such that it is orthogonal to its own translations:

$$\langle g[n-2k], g[n-2l] \rangle = \delta_{kl}, \quad (2)$$

and it is satisfied that $h[n]$ and $g[n]$ are mutually orthogonal

$$\langle h[n-2k], g[n-2l] \rangle = 0. \quad (3)$$

Therefore, an orthonormal set $\{h[n-2k], g[n-2l]\}_{k,l \in \mathbb{Z}}$ is called orthonormal basis in ℓ^2 .

For the biorthogonal case, a low-pass filter \tilde{h} and a high-pass filter \tilde{g} are defined according to:

$$\langle \tilde{h}[n-2k], \tilde{h}[n-2l] \rangle = \delta_{kl} \quad (4)$$

$$\langle \tilde{g}[n-2k], \tilde{g}[n-2l] \rangle = \delta_{kl}, \quad (5)$$

and

$$\langle \tilde{h}[n-2k], \tilde{g}[n-2l] \rangle = \langle \tilde{g}[n-2k], \tilde{h}[n-2l] \rangle = 0. \quad (6)$$

Using the dual basis set \tilde{h} y \tilde{g} and h y g , any sequence in ℓ^2 can be represented as

$$x[n] = \sum_{k \in \mathbb{Z}} \alpha_k \tilde{h}[n-2k] + \sum_{l \in \mathbb{Z}} \beta_l \tilde{g}[n-2l], \quad (7)$$

where

$$\alpha_k = \langle h[n-2k], x[n] \rangle, k \in \mathbb{Z} \quad (8)$$

$$\beta_l = \langle g[n-2l], x[n] \rangle, l \in \mathbb{Z}, \quad (9)$$

and any sequence in ℓ^2 can be represented as

$$x[n] = \sum_{k \in \mathbb{Z}} \tilde{\alpha}_k h[n-2k] + \sum_{l \in \mathbb{Z}} \tilde{\beta}_l g[n-2l], \quad (10)$$

where

$$\tilde{\alpha}_k = \langle \tilde{h}[n-2k], x[n] \rangle, k \in \mathbb{Z} \quad (11)$$

$$\tilde{\beta}_l = \langle \tilde{g}[n-2l], x[n] \rangle, l \in \mathbb{Z}. \quad (12)$$

In Fig. 3 and Fig. 4 are presented the frequency and phase responses of the filters h and g used in this work according to (11) and (12). These filters are near symmetrical, orthogonal and bi-orthogonal

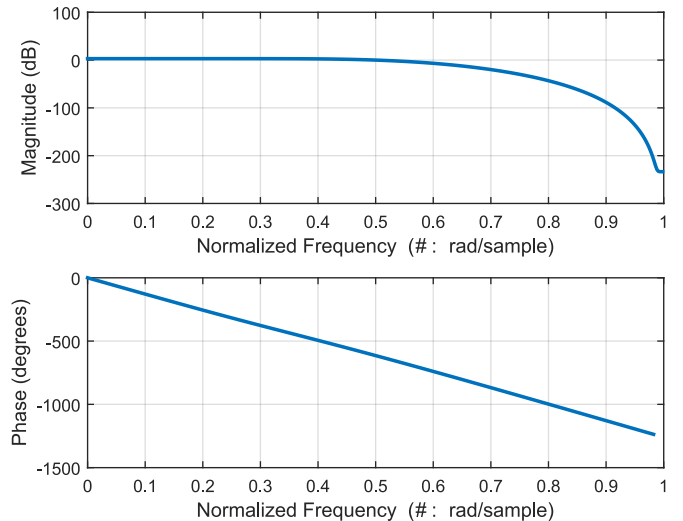


Fig. 3. Low pass frequency and phase response

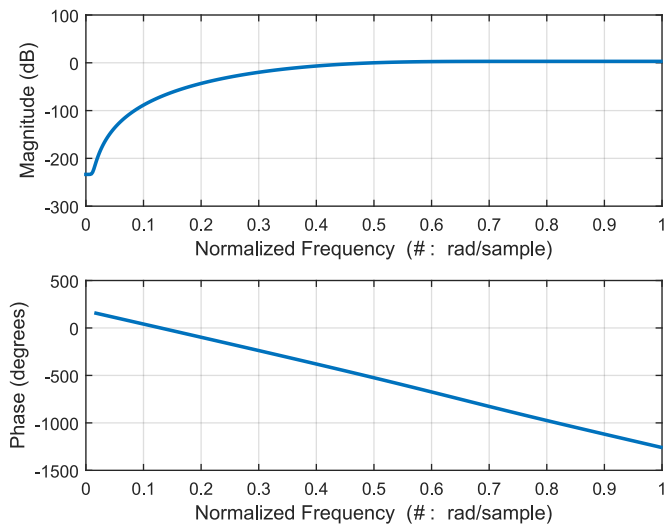


Fig. 4. High pass frequency and phase response

It is noticeable that the band-pass filters are constructed by using the filters shown in Figs. 3 and 4 by applying successive decomposition and dyadic sub-sampling. Therefore, the resulting band-pass filter is constructed from a multi-rate decomposition for the low and high-pass filters.

C. Adaptability criteria

An automatic selection for multi-rate filter banks is applied based on an entropy information criteria. The search of the adequate multi-rate filters is performed by using a depth first search strategy by including a dyadic sub-sample strategy. The selection of the frequency bands is determined by the entropy of the decomposed segment. Since the signal is analyzed by linear sliding windows, the resulting selection of frequency bands is time-varying, based in the information of the decomposition tree. This decomposition is known as best tree selection [18].

The selection of the bands for the classification stage takes into account the similarity of the selected bands during a segment by considering sliding windows. Therefore, even when an adaptive time-varying best tree decomposition is obtained, a fixed band-pass filter is used for each record but considering only the bands that are repeated during the whole interval.

III. RESULTS AND DISCUSSION

A. Data recording and pre-processing

EEG data were collected from one patient with epilepsy who underwent pre-surgical evaluation at the Neurological Center for Epilepsy Treatment and other Neurological Disorders (Neurocentro de Occidente). The ethical committee of Universidad Tecnológica de Pereira approved the study, and the patient gave written informed consent. Data was recorded in six different sessions, consequently, we treat each session as a single database, which comprises about five minutes of each class (epilepsy and normal EEG activity), but including the seizure onset time. Each database was pre-processed independently using the following steps: Data was filtered from 1 to 30 Hz, as suggested in [19] for epileptic activity. Later, Independent Component Analysis (ICA) is performed in order to remove

artifacts. Once data is clean, we created one-second-long epochs that would be used to feed the characterization and machine learning processes. An example of two epochs during normal and pathological conditions, along with the power of each segment projected over the scalp, is presented in Figs. 5 and 6. It is noticeable that the power during both conditions (normal and pathological) is very similar if considering the whole frequency spectrum, and therefore, a selection of bands of interest is required.

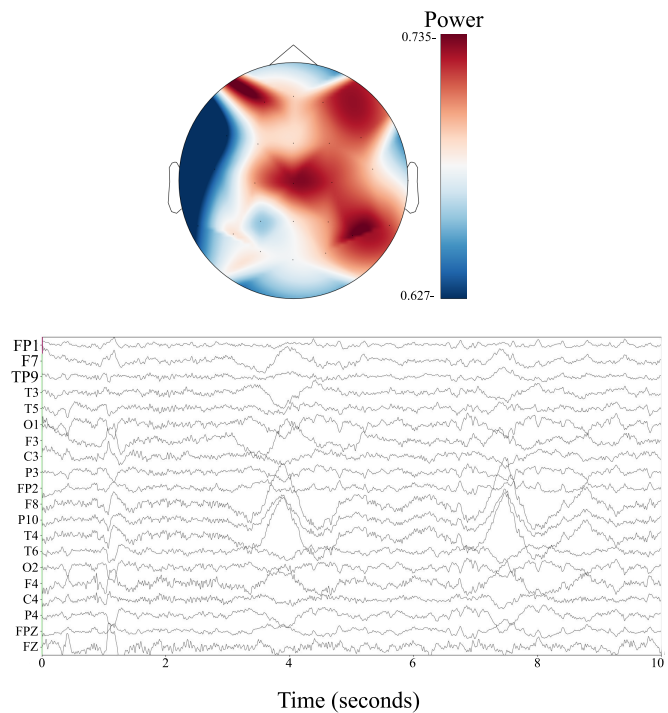


Fig. 5. Example of EEG data in normal conditions

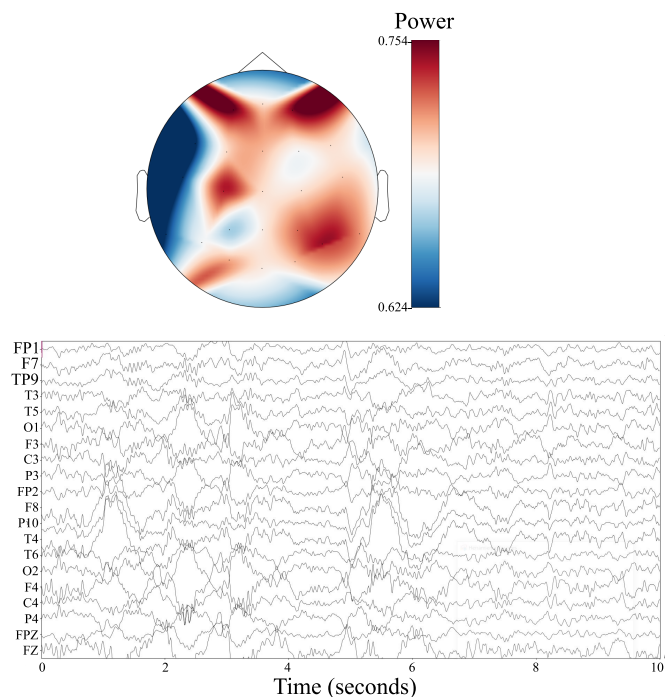


Fig. 6. Example of EEG data in epileptic conditions

B. Tuning of Adaptive Analysis and feature selection

The adaptability scheme consists of selecting, for each EEG segment, an appropriated filter $H_k(z)$ according to the entropy of the spectral information of the analyzed signals. Moreover, as we used a sliding window of 0.5 seconds to cover the whole EEG segment, the resulting multi-rate decomposition is selected in such a way that considers the same distribution of all the analyzed windows. In Fig. 7 are presented the cut frequencies of the selected multi-rate filters.

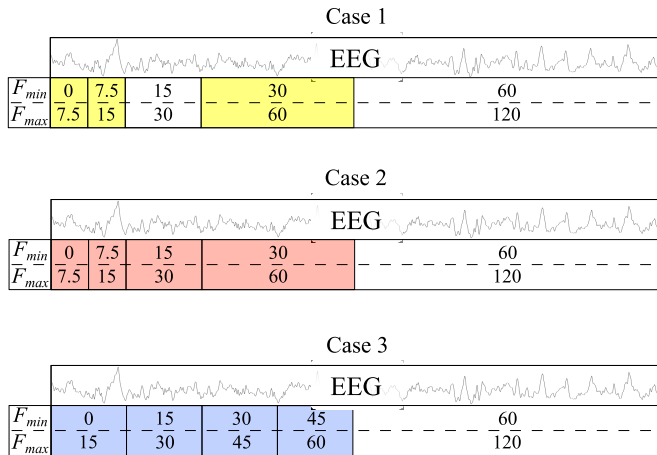


Fig. 7. Cutoff frequencies for the Multi-rate filter banks.

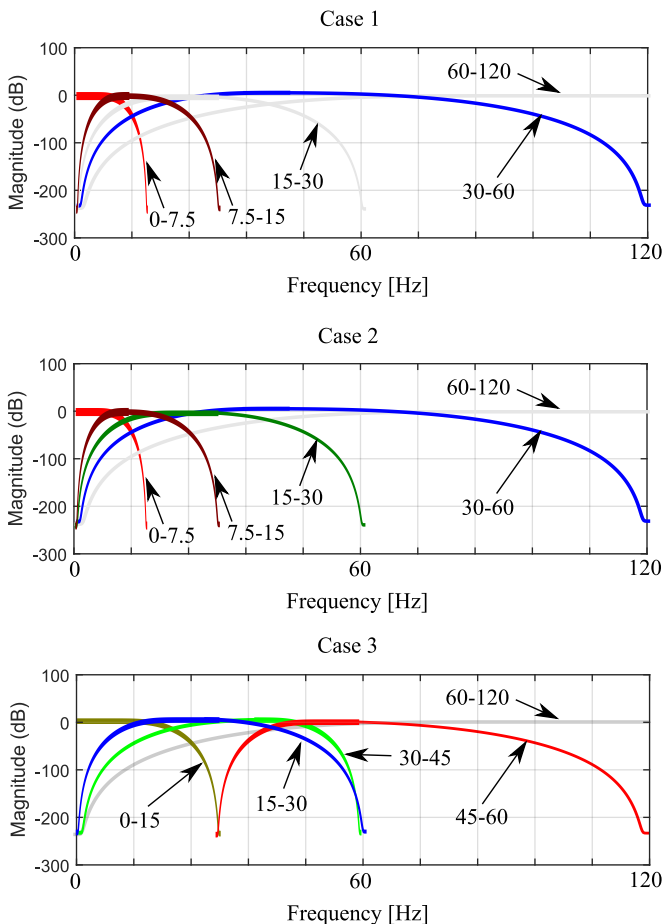


Fig. 8. Multirate passband filters band frequencies responses

Moreover, to look at a feature selection stage, three different multi-rate approaches are used: In the first case, the

selected band-pass filters are the ones that are repeated in all the sliding windows. In the second case, the band-pass filters selected in the first case are increased by completing the spectrum at least to the half of the spectrum (60Hz). Finally, the case 3 includes a decomposition of the segment by using wavelet packets. In Fig. 8 is shown the corresponding frequency responses of the multi-rate filter banks for the three analyzed cases.

In Fig. 9 are summarized the differences between raw and filtered data for normal and epileptic recordings in the power topographical plot for one of the selected frequency bands. It can be seen that when data is processed according to the multi-rate filter banks, differences between normal and epileptic events are highlighted, improving the chance to separate such events using machine learning techniques.

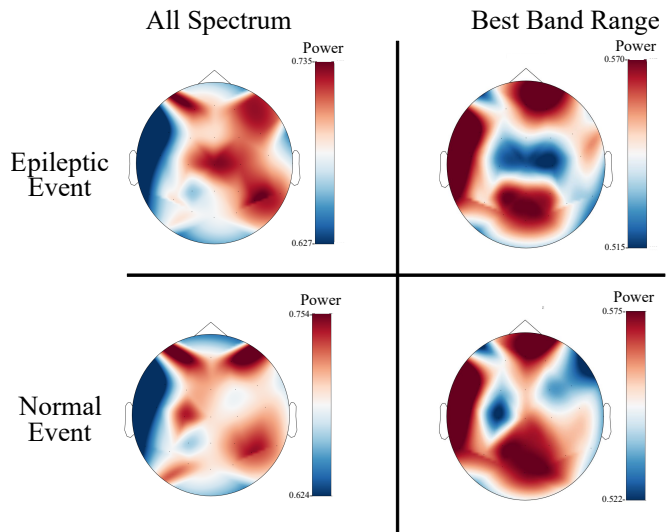


Fig. 9. Differences between raw and filtered data for normal and epileptic recordings

C. Characterization of filtered EEG data

Once each EEG recording has been filtered according to the multi-rate filter bank, we computed several statistical measures to the coefficients of each channel at each frequency band. Namely, we computed the maximum value, minimum value, mean, median, variance, standard deviation, skewness, and kurtosis. Accordingly, for each EEG recording and frequency band, we compute $8 \times N_c$ features, being N_c the number of EEG channels. As a result, for each EEG segment belonging to either normal or epileptic event, the features belonging to all the frequency bands are concatenated into a single vector that will be used as input to the machine learning stage.

D. Classification of epileptic events using Support Vector Machines

Towards discriminating epileptic from normal EEG epochs, we used the statistical features explained above to feed a Support Vector Machine (SVM) classifier with a radial basis function (RBF) kernel. Implementation was done using the Scikit-learn library in Python [20]. As we are more interested in identifying epileptic activity, we used as performance measure the recall that, intuitively, is the ability of the classifier to find all the positive samples. Consequently,

we targeted as positive samples the epochs with epileptic activity. We also used 5-folds cross-validation to search for the best SVM parameters, namely, kernel band-width and regularization. The used grid of values is shown in Fig. 10. The tuning procedure is presented in the form of a heat map, where the parameters c and Γ are selected in terms of the classification performance.



Fig. 10. Example of the used grid to tune the SVM parameters.

E. Classification Results

Tables I, II, and III show the classifications results (mean \pm std) for each of the considered multi-rate decomposition, namely, best band selection, best band with full spectrum, and wavelet packet. As seen, classification was performed individually per frequency band and also combining all the features obtained in each decomposition. As expected for epileptic activity, when seeing independently per frequency band, higher results are obtained in lower bands, namely, 0 – 7.5Hz. This holds for all the considered filter banks. However, the best results are achieved when combining all the available information.

TABLE I
ACHIEVED RECALL WITH MULTI-RATE DECOMPOSITION AND FULL SPECTRUM.

Recall		
Segment	B1 (0 - 7.5 Hz)	B2 (30 - 60 Hz)
1	0.807 (0.037)	0.642 (0.095)
2	0.851 (0.006)	0.828 (0.089)
3	0.791 (0.026)	0.777 (0.098)
4	0.789 (0.037)	0.819 (0.053)
5	0.895 (0.004)	0.895 (0.004)
6	0.812 (0.034)	0.766 (0.127)
Segment	B3 (7.5 - 15 Hz)	All Bands
1	0.736 (0.079)	0.881 (0.004)
2	0.772 (0.042)	0.879 (0.004)
3	0.731 (0.125)	0.879 (0.004)
4	0.798 (0.054)	0.879 (0.004)
5	0.895 (0.004)	0.895 (0.004)
6	0.789 (0.102)	0.879 (0.004)

Moreover, it can be seen that results do not improve when completing the spectrum of the EEG data. Consequently, we can conclude that the best band selection performed by the multi-rate decomposition is able to properly identify the frequency bands with relevant information.

TABLE II
ACHIEVED RECALL WITH MULTI-RATE DECOMPOSITION AND FULL SPECTRUM.

Recall with full spectrum			
Segment	B1 (0 - 7.5 Hz)	B2 (30 - 60 Hz)	B3 (7.5 - 15 Hz)
1	0.807 (0.037)	0.642 (0.095)	0.802 (0.061)
2	0.851 (0.006)	0.828 (0.089)	0.795 (0.053)
3	0.791 (0.026)	0.777 (0.098)	0.732 (0.111)
4	0.789 (0.037)	0.819 (0.053)	0.789 (0.031)
5	0.895 (0.004)	0.895 (0.004)	0.895 (0.004)
6	0.812 (0.034)	0.766 (0.127)	0.784 (0.120)
Segment	B4 (15 - 30 Hz)	All Bands	
1	0.736(0.079)	0.879 (0.004)	
2	0.772 (0.042)	0.879 (0.016)	
3	0.7311 (0.125)	0.879 (0.004)	
4	0.798 (0.054)	0.879 (0.004)	
5	0.895 (0.004)	0.895 (0.004)	
6	0.789 (0.102)	0.879 (0.004)	

Finally, it can be seen that by combining all the information provided by a fixed multi-rate decomposition, as wavelet packet, it is not suitable to identify the relevant information of the process. Consequently, the identification of epileptic activity is not properly carried out. This is evident when seeing the last column of Table III.

TABLE III
ACHIEVED RECALL WITH WAVELET PACKETS AS MULTI-RATE DECOMPOSITION.

Recall Wavelet Packets		
Segment	B1 (0 - 15 Hz)	B2 (15 - 30 Hz)
1	0.795 (0.028)	0.802 (0.061)
2	0.846 (0.009)	0.795 (0.053)
3	0.798 (0.040)	0.732 (0.111)
4	0.825 (0.053)	0.789 (0.031)
5	0.895 (0.004)	0.895 (0.004)
6	0.793 (0.057)	0.784 (0.120)
Segment	B3 (30 - 45 Hz)	All Bands
1	0.731 (0.112)	0.623 (0.188)
2	0.830 (0.032)	0.777 (0.107)
3	0.784(0.062)	0.790 (0.158)
4	0.823 (0.018)	0.597(0.023)
5	0.895 (0.004)	0.544 (0.107)
6	0.800 (0.076)	0.752 (0.004)

IV. CONCLUSIONS

In this work, a methodology to model and describe a set of EEG signals from a patient with epilepsy using time-frequency information through the design and application of adaptive filters is proposed. This methodology allows the adequate description of two classes: normal EEG activity and epileptic seizures. Also, a classification stage by using the proposed method is used to characterize and extract features from the EEG. A comparison with fixed multi-rate filters, as wavelet packet, and by using the full spectrum, information is performed to validate the proposed approach. As a result, the proposed methodology achieves the highest scores in almost all the segments and frequency bands assessed by recall metric to consider the epileptic class as the objective class.

Finally, it is worth noting that the best results are achieved when all the available information among the several frequency bands are considered.

REFERENCES

[1] A. Alkan and A. Subasi, "Automatic seizure detection in eeg using logistic regression and artificial neural network," *Journal of Neuroscience Methods*, 2005.

- [2] A. Schad, K. Schindler, and B. Schelter, "Application of a multivariate seizure detection and prediction method to non-invasive and intracranial long-term eeg recordings," *Journal of Neuroscience Methods*, 2005.
- [3] A. Sreekumar, A. Sasidhar Reddy, D. Udaya Ravikanth, M. Chaitanya Chowdary, G. Nithin, and P. Sathidevi, *Epileptic Seizure Detection Using Machine Learning Techniques*, 2021, vol. 668.
- [4] M. A. Colominas, M. E. S. H. Jomaa, N. Jrad, A. Humeau-Heurtier, and P. Van Bogaert, "Time-varying time-frequency complexity measures for epileptic EEG data analysis," *IEEE Transactions on Biomedical Engineering*, vol. 65, no. 8, pp. 1681–1688, 2018.
- [5] M. Bueno-Lopez, E. Giraldo, M. Molinas, and O. Fosso, "The mode mixing problem and its influence in the neural activity reconstruction," *IAENG International Journal of Computer Science*, vol. 46, no. 3, pp. 384–394, 2019.
- [6] A. Takajyol, M. Katayamal, and K. Inoué, "Time-frequency analysis of human sleep eeg," *SICE-ICASE International Joint Conference 2006*, 2006.
- [7] C. Bigan and M. Woolfson, "Time-frequency analysis of short segments of biomedical data," *IEE Proc-Sci. Meas. Techno. Vol. 147, No. 6, November 2000*, 1995.
- [8] J. D. Martinez-Vargas, E. Giraldo, and G. Castellanos-Dominguez, "Enhanced spatio-temporal resolution using dynamic sparse coding for eeg inverse problem solutions," *IAENG International Journal of Computer Science*, vol. 46, no. 4, pp. 564–574, 2019.
- [9] M. Bueno-Lopez, P. A. Munoz-Gutierrez, E. Giraldo, and M. Molinas, "Electroencephalographic source localization based on enhanced empirical mode decomposition," *IAENG International Journal of Computer Science*, vol. 46, no. 2, pp. 228–236, 2019.
- [10] Y. Yang, "Empirical mode decomposition as a time-varying multirate signal processing system," *Mechanical Systems and Signal Processing*, vol. 76-77, pp. 759 – 770, 2016. [Online]. Available: <http://www.sciencedirect.com/science/article/pii/S088832701600073X>
- [11] G. Piella and B. Pesquet-Popescu, "Adaptive wavelet decompositions driven by a weighted norm of the gradient," *Proc. 3rd IEEE Benelux Signal Processing Symposium*, Belgium 2002.
- [12] —, "Content adaptive multiresolution analysis," *Proceedings of Acivs 2004 (Advanced Concepts for Intelligent Vision Systems)*, Belgium 2004.
- [13] R. L. Claypoole, R. G. Baraniuk, and R. D. Nowak, "Lifting constructions of non-linear wavelet transforms," *IEEE transactions on image processing*, vol. 12, no. 12, pp. 1449–1459, January 2003.
- [14] H. Heijmans, B. Pesquet-Popescu, and G. Piella, "Building nonredundant adaptive wavelets by update lifting," *Applied and Computational Analysis*, vol. 18, no. 4, pp. 252–281, January 2005.
- [15] H. Heijmans and G. Piella, "Adaptive lifting schemes with perfect reconstruction," *IEEE Trans. Signal Processing*, vol. 50, no. 7, pp. 2204–2211, January 2003.
- [16] Z. Duan, J. Zhang, C. Zhang, and E. Mosca, "A simple design method of reduced-order filters and its applications to multirate filter bank design," *Signal Processing*, vol. 86, no. 5, pp. 1061 – 1075, 2006. [Online]. Available: <http://www.sciencedirect.com/science/article/pii/S0165168405002537>
- [17] S. Cao, "Spike train characterization and decoding for neural prosthetic devices," *California Institute Of Technology*, 2003.
- [18] G. Strang and T. Nguyen, *Wavelets and Filter Banks*. Wellesley, MA, USA: Wellesley-Cambridge Press, 1996.
- [19] A. Sohrabpour, Z. Cai, S. Ye, B. Brinkmann, G. Worrell, and B. He, "Noninvasive electromagnetic source imaging of spatiotemporally distributed epileptogenic brain sources," *Nature communications*, vol. 11, no. 1, pp. 1–15, 2020.
- [20] F. Pedregosa, G. Varoquaux, A. Gramfort, V. Michel, B. Thirion, O. Grisel, M. Blondel, P. Prettenhofer, R. Weiss, V. Dubourg, J. Vanderplas, A. Passos, D. Cournapeau, M. Brucher, M. Perrot, and E. Duchesnay, "Scikit-learn: Machine Learning in Python," *Journal of Machine Learning Research*, vol. 12, pp. 2825–2830, 2011.